Colloid & Polymer Science Colloid Polym Sci 271:1024–1034 (1993)

Structural analysis of anisometric colloidal iron(III)-hydroxide particles and particle-aggregates incorporated in poly(vinyl-acetate) networks

W. Haas, M. Zrinyi*), H.-G. Kilian, and B. Heise

Abteilung Experimentelle Physik, Universität Ulm, FRG
*) Department of Physical Chemistry, Technical University of Budapest, Hungary

Abstract: Anisometrical colloidal iron(III)hydroxide particles and particle aggregates were incorporated in elastic poly(vinyl acetate) networks. A novel method has been developed to fix the colloidal structure of deformed samples. Digitalized image analysis has been applied in order to evaluate the micrographs. The rod-like particles allow for studying the local deformation and orientation due to uniaxial and triaxial deformations. The density correlation function as well as the micrographs show that the structure of aggregates is not influenced by the strain. Due to strong attractive interactions between the colloidal particles the developing strain is not enough to destroy the aggregate structure. The orientation behavior of the model filled networks can be satisfactorily described by using the affinity principle.

Key words: Filled networks – TEM – fractal aggregates – uniaxial and triaxial deformations

Introduction

It is well established that significant improvements in both elastic and swelling properties of networks can be made by the incorporation of filler particles [1–6]. The traditional method of preparing filled elastomers by the technique of blending of a finely divided filler (most notably carbon black or silica) into a polymer before cross linking has a significant disadvantage. In most cases instead of individual particles, aggregates are present and their size distribution cannot be controlled. A novel method for preparing filled elastomeric networks was developed by Mark et al. [7–9] by precipitating well-dispersed particles of silica in the polymeric material. The "in situ" precipitation can be made before, during and after the cross-linking reaction.

In this paper, we report a different method of preparing filled networks [10]. The preparation and characterization of colloidal filler particles is made separately from the cross-linking reaction. By this means, not only individual particles, but also aggregates can be used as model filler particles. The advantage of this method is that we can control the concentration of filler particles, furthermore, the size of aggregates can also be varied.

One of the main purposes of the present work is to report on the sample preparation. Special attention is paid to sample arrangement for transmission electronmicroscopical investigations. By using this method the effects of swelling and unidirectional deformation on the distribution and orientation of colloidal iron(III)-hydroxide particles are studied. The rod-like filler particles were considered as indicators of local deformation and orientation.

Experimental

1. Preparation of iron(III) hydroxide sol

The iron(III) hydroxide sol was prepared from iron(III) chloride and ammonium carbonate (Reanal, Hungary). As suggested by Graham [11], 100 cm^3 of iron(III) chloride solution (concentration: 35 mass-%) was mixed carefully with 30 g

ammonium carbonate dissolved in distilled water (concentration: 37 mass-%). The reaction took place under intensive stirring. After the reaction was finished, the mixture was dialyzed against water in order to get rid of the remnants of mobile ions. The dialysis took 4 weeks. The equilibrium dispersion medium of the sol was analyzed after centrifuging the solid particles from the sol by ultracentrifuge. It was found to be equivalent with 10^{-4} M HCl solution. The medium was used as diluent to obtain sols of different concentrations. In aqueous solution, the surface of an iron(III) hydroxide sol particle is positively charged. The charge density was found to be $\sigma_0 = 86\ \mu C\,cm^{-2}$. For the surface potential (ψ_0) a value of 259 mV was obtained. The iron(III) hydroxide particles are not spherical. It will be shown later that the rod-like particles have a long axis of 20–30 nm and a width of 2–3 nm. Thus, a mean aspect ratio of 10 can be used to characterize the anisometry.

2. Preparation of chemically cross linked PVA networks filled with iron(III) hydroxide sol (IS) particles

PVA is a neutral polymer, which reacts under certain conditions with glutaraldehyde (GDA) [12]. The crosslink density can conveniently be varied by the amount of GDA. In this work, the ratio of vinyl alcohol monomer units (VA) of PVA to the amount of GDA was kept constant, [VA]:[GDA] = 300:1. The PVA (Merck, FRG) was hydrolyzed in order to remove the small amount of vinyl acetate groups on the chains. The hydrolysis was followed by repeated precipitation and dissolution, in order to narrow the molar-mass distribution. After fractionation and purification, the polymer was carefully dried, and dissolved again in the equilibrium medium of the IS sol. The concentration of IS particles was varied by diluting the PVA solution with different amounts of IS sol.

After mixing the PVA solution with IS sol, 2 days were allowed for the adsorption equilibrium to be attained. The cross linking agent (GDA) was then introduced into the system. Reaction was induced by decreasing the pH of the system below 2.5. Hydrogen ions catalyze the reaction. The total volume of reaction mixture, as well as the amount of PVA were always the same. Thus, the networks were prepared at a fixed initial polymer concentration. The comparatively slow reaction (2–6 h) enabled us to fill a suitable mold, to obtain gels of defined shape. After a reaction had finished, a gel was taken out of the mold and washed several times with the equilibrium medium in order to remove traces of unreacted matters.

With the aid of a procedure described here, individual colloid particles were built into the network. If the sol was coagulated before mixing it with the polymer solution, then, due to the attraction forces between particles, aggregates form. The aggregates could also be incorporated into the polymer matrix using the same procedure, but instead of the sol, a suspension of coagulated IS particles was used.

3. Preparation of filled poly(vinyl acetate) (PVAc) networks

The PVAc networks were prepared by acetilation of PVA gels in a mixture of pyridine (50 vol%-acetic acid (10 vol%)-acetic anhydride (40 vol%) at 90 °C for 8 h [12]. The acetilation mixture was renewed hourly. In the last 3 h the acetic acid was omitted from the fresh mixture in order to shift the equilibrium in the direction of acetate formation. After the reaction had been completed, the gel media were replaced by acetone. Several solvent exchanges, each taking 48 h or more, were made in order to get rid of the reaction mixture as well as other soluble components. After the solvent exchanges the gels were carefully dried. It must be mentioned that during the acetylation reaction the iron(III)-hydroxide particles have not dissolved. A comparison of TEM photographs made before (in PVA) and after the acetilation reaction (in PVAc) shows no definite difference as far as the shape and size of iron(III) hydroxide particles are considered [10].

4. Electron microscopy and image processing

Transmission electron micrographs are obtained by taking advantage of the different scattering of electrons on passing sample areas of different composition. Discrimination of inelastically and elastically scattered electrons in imaging is possible by the Zeiss EM 902 transmission electron microscope. This is achieved by a prism-mirror-prism energy loss spectrometer, which is

integrated into the optical axis of the microscope [13]. The electrons are deflected and discriminated according to their energy by means of a magnetic prism. An electrostatic mirror and a second magnetic prism are used to bring the electrons back into the optical axis. The strength of the magnetic prism is chosen such that electrons having energy of 80 keV are deflected twice, by exactly 90°.

Electrons of different energy can be faded out by a slit diaphragm below the double prism. Increasing the acceleration voltage up to 2000 V allows to tune specific inelastically scattered electrons into the optical axis (energy loss compensation). Thus, an image can be formed either from elastically or from specific inelastically scattered electrons. There are two major advantages of this technique. The chromatic aberration due to different focusing of elastically and inelastically scattered electrons can be eliminated. The local resolution and the contrast are improved by imaging using only the elastically scattered electrons (elastic bright field imaging).

The Zeiss EM 902 works with an accelerating voltage of 80 kV and hair pin tungsten filament as an electron source. The electron micrographs were obtained by elastic bright field imaging. Image processing was accomplished with the IBAS 2000 image processing system of Kontron.

5. Preparation of filled PVAc networks for electronmicroscopical investigation

One of our main aims is to study the effect of deformation on the local orientation of rod like IS particles as well as on the structure of aggregates in the PVAc matrix. To realize this purpose, one needs to both fix the deformed samples in order to maintain the constant strain, and to prevent the possible orientation due to cutting the sample for TEM investigations. Several attempts have been made to solve this problem. Additional crosslinking of deformed PVAc networks by γ-rays, as well as cooling down below the glass temperature ($T_g = 38\,^{\circ}C$) have been performed with unsatisfactory results.

A new method has been introduced by means of which several deformation modes can be applied, and immobilized. The PVAc networks can swell in low-viscosity epoxy-resin-acetone mixture. The swelling degree can be convieniently varied by the concentration of acetone in the mixture. The PVAc networks can swell in this mixture, then by increasing the temperature upto 70 °C, a cross-linking polymerization takes place. In order to avoid the evaporation of acetone and other components, this procedure is led in a closed vessel. The cross-linking polymerization takes 24 h. As a result of this, an interpenetrated network (IPN) of PVAc and epoxy polymer comes into existence. Due to incompatibility between polymers not every type of epoxy resins can be used. The best results have been obtained by using the following epoxy trunk solution: EPON 812 43.2 mass% 2-dodecenylsuccinic anhydride 37.5 mass%, methylnadic anhydride 17.8 mass% and 2,4,6-tris(dimethylaminomethyl) phenol 1.5 mass%. All of these materials were purchased from SERVA. This trunk solution was mixed with acetone. The presence of epoxy in IPN networks provides the hardness and resistance of the materials used. It is important to mention that prepared samples had no pores at all.

Two kinds of experiments have been realized. We have prepared equitriaxially deformed samples by using the epoxy solution as a swelling agent. In addition, unidirectional extension was carried out by deforming the polymer swollen to lower degrees. Polymerization of the swelling agent was then carried out at constant strain.

Ultrathin specimens were obtained by trimming the dry network to a suitable shape and microtoming with a diamond knife using an ultramicrotome (Reichert–Jung) at room temperature. The thickness of the specimen was 50–100 nm, indicated by their silvery to golden interference.

Results and discussion

1. Distribution of filler particles in the PVAc network

In this section some electron micrographs are presented in order to show the applicability of technique developed by us.

Figure 1 shows the distribution of IS particles in the PVAc matrix at two different magnifications. In this case, stable colloidal IS particles were incorporated in the polymer matrix. One can see that on large length scale the distribution of particles is homogeneous. It is worth mentioning,

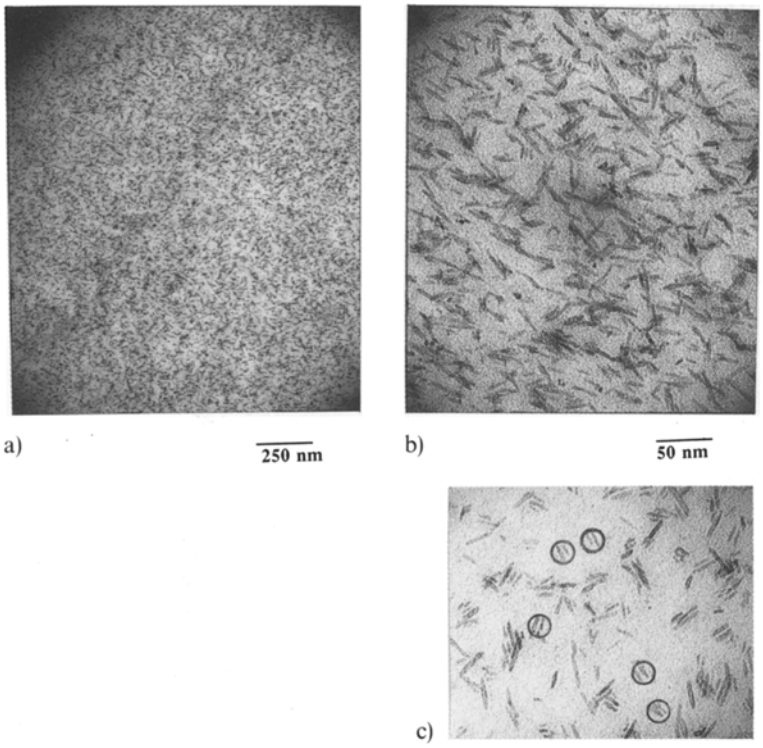

Fig. 1. Distribution of colloidal IS particles in the PVAc network. Stable IS particles were incorporated in the polymer. 1c shows doublets and triplets denoted by circles

beside the individual particles, small clusters containing 2–5 rods can also be seen. This is well demonstrated by Fig. 1.c which shows this phenomenon considerably. In the figure some dimer and trimer are indicated by circles. It is important to emphasize that most of the small aggregates consists of rods which are parallelly packed and forming small bundles. It can be seen that the particles in the bundles are separated by a certain distance and one can suppose that the space between the parallel IS particles is filled by polymer chains. It is very likely that a reversible aggregation occurs in the stable sol due to the secondary minimum of the DLVO potential [14, 15, 16]. Maeda and Hachisu have found that Schiller layer from anisometric β-ferric oxyhydroxide sol can be observed by the naked eye, even in the case of stable sol [16]. On the basis of DLVO theory developed for rods, they found that both attractive interactions as well as the repulsive interactions together with the secondary minimum give the parallel orientation an advantage.

Figure 2 shows the structure of IS aggregates. In this case no stable sol particles were mixed with the polymer solution, but aggregates which formed as a result of attractive interactions due to the presence of electrolytes. One can see the basic difference in the particle distribution. Now, the rod-like IS particles overlap each other, while in the stable colloid system, the number of attached particles is much smaller. It is obvious that distribution of filler particles can be controlled to a great extent by the ionic strength during the preparation process.

We have also found that the initial particle concentration makes its influence felt on the average size of aggregates. If the coagulation is performed in dilute solution, then the resulting aggregates have larger dimensions. As an illustrative example, Fig. 3 demonstrates this effect. As the initial concentration of particles increases, the average size of aggregates decreases. The difference in average size can be several orders of magnitude. This finding has been supported by recent viscosity and settling velocity measurements [17].

2. Evidence for the fractal structure of anisometric IS particle aggregates

As we have seen in Figs. 1–3, the flocculated iron(III)-hydroxide sol particles show a tenuous and ramified appearance. One can observe that

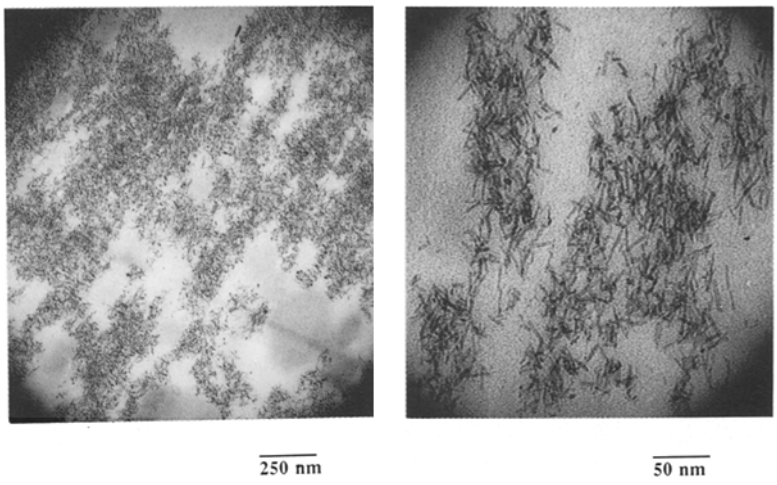

Fig. 2. Aggregates of IS particles in the polymer matrix. The sol was coagulated before mixing it with the polymer solution

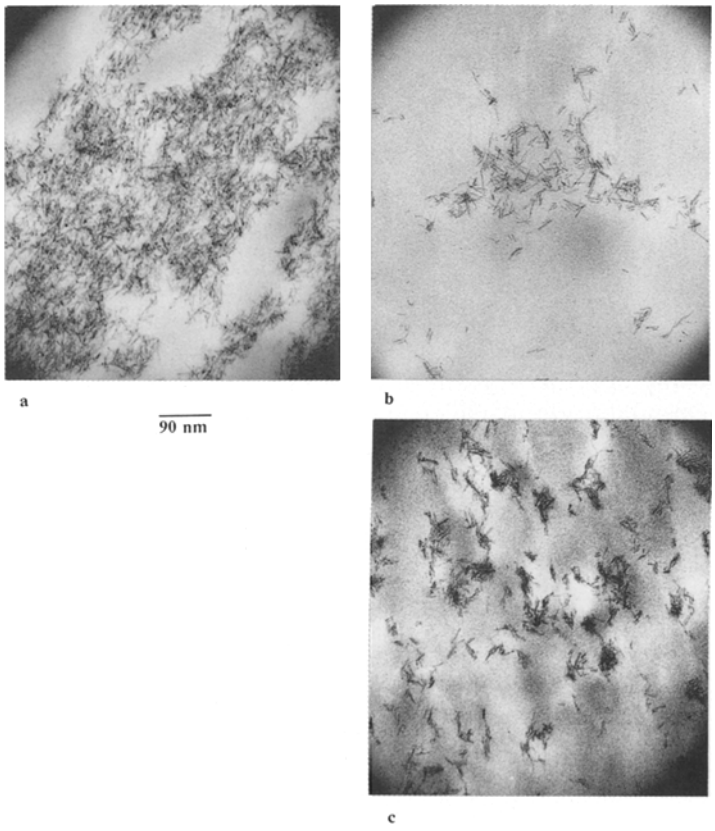

Fig. 3. The effect of initial particle concentration on the size of aggregates. The volume fraction of sol particles was a: 0.0091; b: 0.044; c: 0.084. The coagulation was performed at the same ionic strength

there exists strong visual similarity between IS particle-aggregates and simulated images of different cluster-cluster aggregation models [18, 19]. The common feature of clustering of cluster models, is that they provide fractal objects. In case of a volume fractal one defines the fractal dimension, D which quantitatively measures the more or less rugose aspect of the object. If one determines the mass contained in a sphere of radius, r centered at a given point of the object, then this

mass, $m(r)$ scales with the distance as r^D, where the fractal dimension, D is usually non-integer and smaller than the embedding dimension.

We have made a two dimensional image analysis in order to establish whether the IS aggregates show fractal character, or not. The fractal dimension was determined by the successive squares method [20]. The center of gravity of the largest aggregate on the electron micrograph was picked as the center of a series concentric squares of different edge, l. It was assumed that the number of pixels is in direct proportion to the number of particles in each choosen square. The number of pixels within each square $N_P(l)$ was counted. Figure 4 shows the log-log plot of $N_P(l)$ versus l for an aggregate. From the slope $D_s = 1.5$ was obtained. It must be mentioned that D_s is not the fractal dimension of the whole aggregate. For the electronmicroscopical studies usually a layer of 50–100 nm thickness are cut. Since the size of our selected aggregate is much larger than the layer thickness, what we see is not a two-dimensional projection, but a slice from the aggregate. It is obvious that this part of the aggregate has a definite fractal character. The problem however remains for the determination of volume (mass) fractal dimension, D from D_s. It must be mentioned that the effect of particle anisotropy on the fractal dimension has not been studied as yet.

3. Effect of swelling on the average distance between particles

In order to study the local deformation of filler particles in networks, swelling experiments were made. From a macroscopical point of view swelling can be considered as an equi-triaxial deformation. By measuring the average distance among the particles as a function of swelling degree one can learn the affine or non-affine character of the deformation. The different swelling degrees were obtained by using epoxy resin-acetone mixture as swelling agent at different concentrations. After the swelling equilibrium had been achieved, the volume have been fixed by the cross-linking reaction of the mixture. Figure 5 shows the effect of swelling on the particle distribution in case of individual particles. All three photos have been made by the same magnifications (30 000). One can see that the random distribution of particles and small aggregates has not been strongly influenced by swelling. If one examines the particle distribution closely, then it becomes obvious that the affine deformation is maintained only on length scales significantly larger than the size of individual particles or particle aggregates. Those particles that are close to each other remain together after the swelling. This is much more emphasized in Fig. 6, where aggregates are shown at different degrees of swelling. It can be seen that

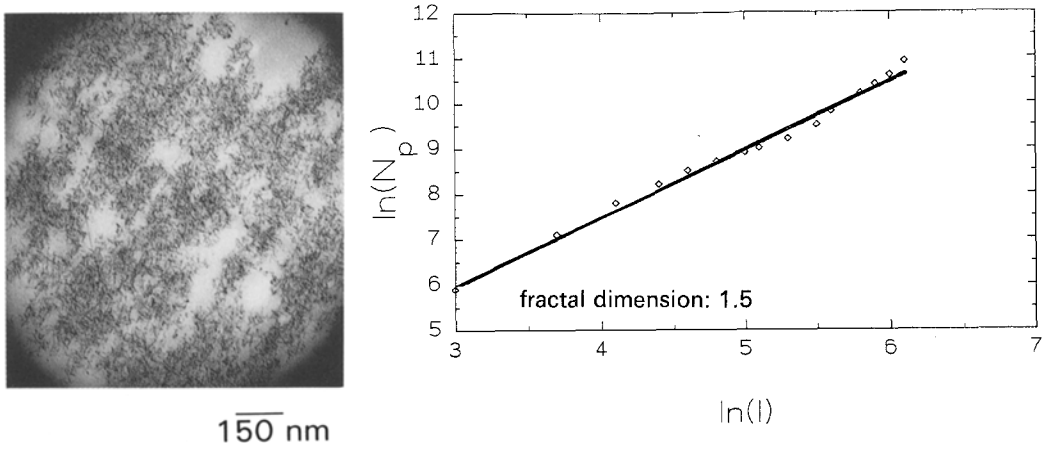

Fig. 4. Evidence for the fractal geometry of an IS aggregates. The slope of the log-log plot provides the fractal dimension $D_s = 1.5$

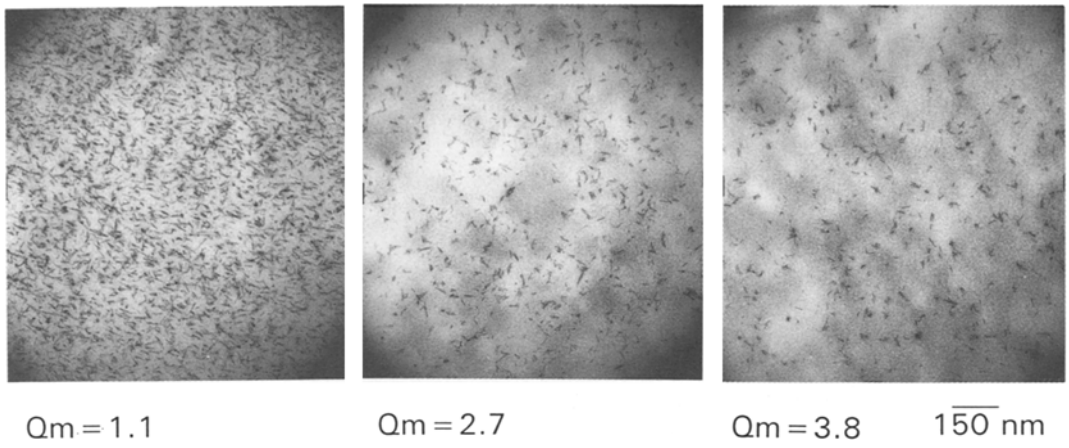

Fig. 5. The effect of swelling on the average distance between the particles. The photos show stable colloidal particles. The swelling degree, Q_m, is expressed as the mass of the interpenetrating filled network divided by the mass of filled PVAc network

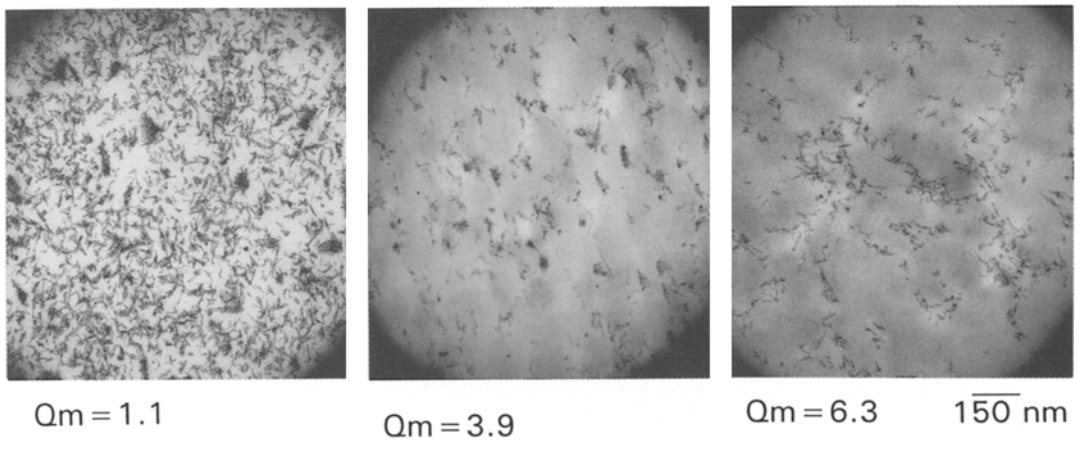

Fig. 6. Swelling of networks containing aggregates.

the affine deformation during equitriaxial deformation does not hold at short length scales. This visual observation is supported by the density-correlation function, shown in Fig. 7. This function provides the probability of finding a particle from a given distance from another one. In case of homogeneous distribution this function has a constant value independent of the distance. The density correlation function was determined with the aid of digitialized images. The position of each particle was characterized by its geometrical focal point. Then, the correlation function was determined by the standard method. Figure 7 shows the density correlation function for the stable sol particles at two different swelling degrees. One can see a maximum on the correlation function at distances between 20–30 nm. This maximum is due to the presence of small bundles formed from IS particles during preparation. What is important for us is that this maximum does not disappear nor does it shift to higher values as a result of swelling. This means again that the deformation of filled networks is not homogeneous. This is a consequence of strong interactions among the particles in aggregates. The stress developed during swelling is not enough to destroy the aggregates and to move the particles away.

4. Effect of strain on the orientation of rod-like filler particles

Up to this point the orientation of rod-like IS particles has not been important because the equitriaxial deformation does not make its influence

felt on the orientation. This is not the case for uni-axial deformation. Due to anisometry, the colloidal iron(III)-hydroxide particles can be used as indicators of local orientation. Samples were prepared in order to see the effect of macroscopic strain on the orientation of particles. The filled PVAc networks first were allowed to swell in the epoxy resin, then it was followed by an unidirectional extension. The deformation ratio (length in deformed state/length in rest state) was $\lambda = 4.1$. Figure 8 shows the orientation of the particles in case of stable sols.

Two magnifications are presented in order to emphasise the effect of deformation. A comparison can also be made with the aid of undeformed samples.

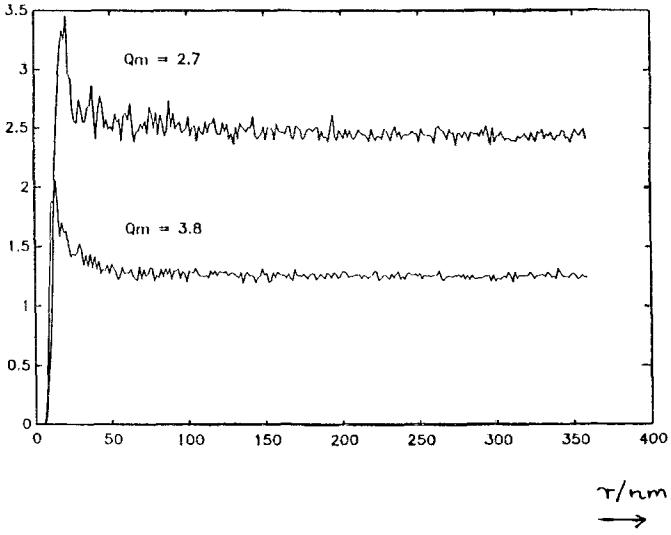

Fig. 7. The density correlation function determined at two different swelling degree denoted in Fig. 5

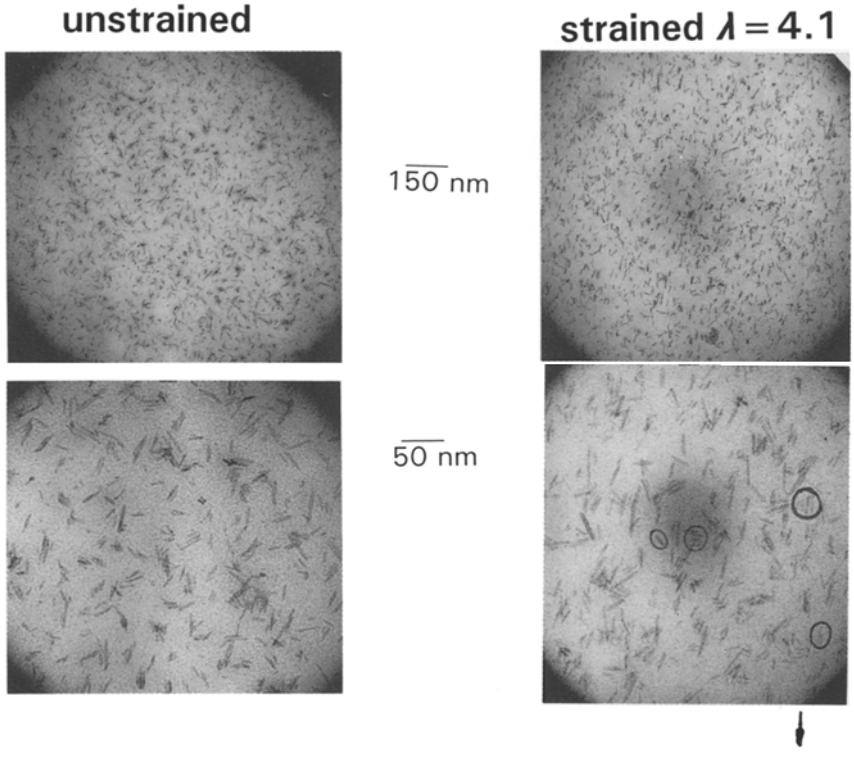

Fig. 8. Orientation of IS particles due to deformation

Before going into detail the following remarks must be made: So far the micrographs which present the structure of individual particles or aggregates in unstrained polymer network show no significant orientation of the particles. The random orientation seems to not be disturbed by microtoning, when preparing the samples for electronmicroscopical investigations. To establish the influence of cutting direction on the particle orientation several experiments were performed.

4.1. Effect of microtoming on the orientation studied by transmission electron micrographs and electron diffraction

In order to make sure that the influence of cutting is not significant, the following experiment was performed: for deformed and undeformed samples the direction of cutting was systematically varied and compared with the transmission electron micrographs. No definite orientation due to cutting could be observed, as shown in Fig. 9. This figure shows the effects of cutting on unoriented and oriented samples. In the case of Figs. 9a and c the direction of microtoming and deformation is perpendicular, while in Figs. 9b and d the two directions are parallel. One cannot see any significant difference between the two situations.

An independent confirmation of particle orientation due to strain can be realized by electron diffraction. To perform such an experiment one needs no preliminary procedure to influence the orientation of solid particles in the elastic matrix.

We have learned from the previous experiments, that if particle orientation takes place, then it is certainly due to the strain.

4.2. Quantitative interpretation of orientation phenomenon on the basis of affine deformation

Figure 8 shows considerably orientation of IS particles in case of deformed polymer. This orientation can be seen by the naked eye. One can also see that there is a remarkable difference in the orientation behavior of single particles, doublets, triplets and small aggregates. The orientation of small aggregates has been found to occur to a lesser extent than for single particles.

A quantitative evaluation can be realized if one measures the angle, ϑ between the longer axis of

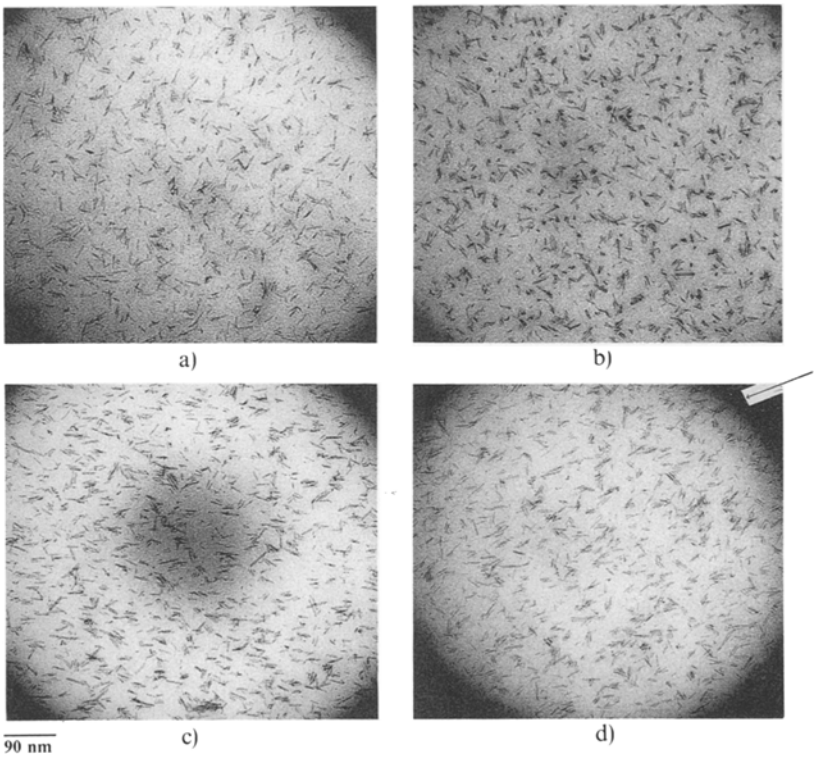

Fig. 9. The effect of microtoming on the orientation of undeformed (a, b) and deformed (c, d) samples. In the case of Figs. 9a and b the direction of microtoming and deformation is perpendicular. For Figs. 9c and d the two directions are parallel. The deformation is chracterized by $\lambda = 4.1$. The arrow indicates the direction of strain

particles and the direction of strain for each particle (in case of full orientation $\vartheta = 0°$), while in other cases one can find angles between $0 < \vartheta < 90°$. Figure 10 shows a typical orientation function where the number of particles having angles between ϑ and $\vartheta + 10°$, $N(\vartheta)$ is plotted as a function of ϑ. One can see that the number of particles belonging to a certain angle domain decreases significantly as ϑ increases. It is useful to define the orientation density distribution function $\rho(\vartheta, \lambda)$, which characterizes the orientation due to deformation. Here, λ denotes the length of the deformed sample relative to the undeformed length measured in the direction of strain. It is defined as the probability of finding an angle between ϑ and $\vartheta + d\vartheta$ at a certain deformation, λ.

If the particles are orientated at random (this is the case at $\lambda = 1$), then $\rho(\vartheta, \lambda) = 1$, in other cases $\rho(\vartheta, \lambda) < 1$.

Taking into consideration the affine deformation of elastic matrix for infinite long, rigid rods, it was found that [21]:

$$\rho(\vartheta, \lambda) = \frac{\lambda^3}{(1 + (\lambda^3 - 1)\sin^2 \vartheta)^{3/2}} \cdot \tag{1}$$

Later, this expression was generalized in order to take into account the finite size of the rigid anisometric particles [22]:

$$\rho(\vartheta, \lambda) = \frac{\lambda^a}{(1 + (\lambda^a - 1)\sin^2 \vartheta)^{3/2}}, \tag{2}$$

where the exponent a is related to the aspects ratio, k according to the following equation:

$$a = 3\frac{(k^2 - 1)}{(k^2 + 1)}. \tag{3}$$

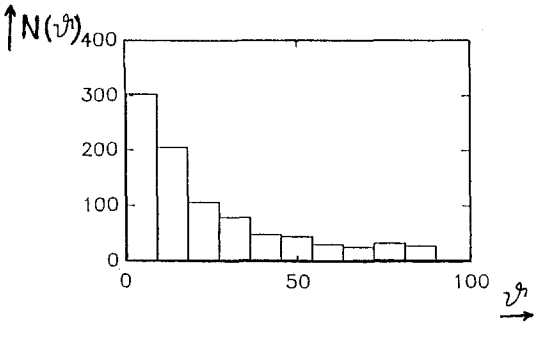

Fig. 10. The orientation distribution function measured at $\lambda = 4.1$

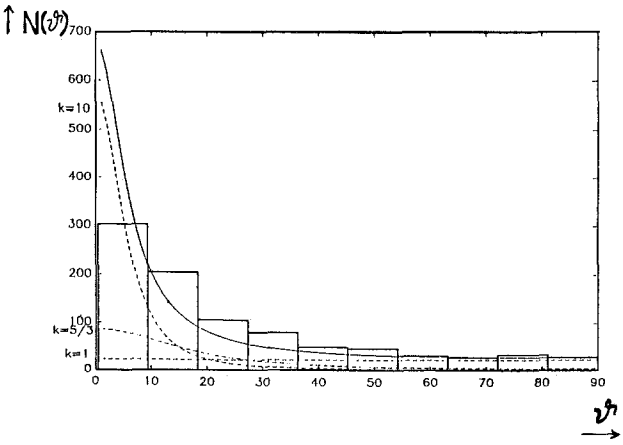

Fig. 11. Comprison of experimental data with the prediction based on the affine deformation. The dotted line represents the dependence given by Eq. (2) for aspects ratio denoted in Fig. 1. The solid line is the sum of the three functions

With the aid of Eqs. (2) and (3), one can compare the experimental data with the theory, and it becomes possible to establish how affine the deformation is. A comparison is made in Fig. 11. Instead of $\rho(\vartheta, \lambda)$ function, $N(\vartheta, \lambda) = \rho(\vartheta, \lambda)\, N_T$ is plotted against ϑ. Here, $N_T = \sum_\vartheta N(\vartheta)$ stands for the total number of particles. Thus, $N(\vartheta, \lambda)$ means the number of particles having angles between ϑ and $\vartheta + d\vartheta$. We know that not only individual particles but also dimers and trimers are present with different aspects ratio. According to our rough estimation, based on the electron micrographs, the proportion among singlets, doublets, and triplets can be given as 2:1:1. The corresponding aspects ratios may be approximated to be: 10, 5/3 and 1.

Figure 11 shows the dependence of $N(\vartheta, \lambda = 4.1)$ on ϑ situation (dotted lines). It can be seen that aspects ratio plays an important role. The solid line represents the sum of the three curves. One can conclude that deviation between experimental results and theoretical prediction is not very significant, that is the orientation of IS particles in the elastic PVAc network seems to be affine.

Conclusion

We have developed a method by means of which the local deformation and orientation can be studied. Anisometrical colloidal particles were

used as indicators of motion at nm length scales. The structure of deformed samples was fixed by producing an interpenetrated network which provides hardness of the samples. Unidirectional and equitriaxial(swelling) experiments were performed and the distribution and orientation of particles was followed by transmission electron microscopy. A digitalized image analysis made possible the quantitative evaluation of data. It was found that

- even the stable sol contains doublets and triplets in a certain amount;
- the interactions between the colloidal particles are so strong that the developing strain during swelling cannot destroy the structure and, as a result of this, the deformation in short scales is no longer affine,
- the orientation of rod-like particles can be described in terms of affine deformation, and the strong influence of aspects ratio on orientation was evidenced;
- a layer from a huge aggregate was analyzed and it was found to be fractal with a dimension of 1.5.

The study of events in filled networks on colloidal length scales should significantly contribute to our understanding of the basic properties of a filled system. The elastic and swelling properties in connection with the structural analysis will be published in a forthcoming paper.

Acknowledgement

It is a great pleasure to acknowledge that one of the authors (M.Z.) has been supported by grants from the Alexander von Humboldt Foundation. This work was partly supported by the SFB 239 and by the Hungarian Academy of Sciences (OTKA No: 2166).

References

1. Hepburn C, Reynolds RJ (1979) Elastomers: Criteria for Engineering Design. Applied Science Publishers
2. Kraus G (1963) Journal of Applied Polymer Science 7:861
3. Kilian H-G (1987) Colloid and Polymer Science 265:410
4. Kilian H-G (1987) Progr Colloid Polym Sci 75:213
5. Kilian H-G, Schenk H (1988) J Appl Polym Sci 35:345
6. Horkay F, Geissler E, Hecht A-M, Pruvost P, Zrinyi M (1991) Polymer 32:835 (1991)
7. Mark JE, Pan S-J (1982) Makromol Chemie, Rapid Comm 3:681
8. Mark JE (1985) British Polymer Journal 17:144
9. Mark JE, Erman B (1988) Rubberlike elasticity a molecular primer. John Wiley & Sons, New York, Chichester, Brisbane, Toronto, Singapore
10. Zrinyi M, Kilian H-G, Dierksen K, Horkay F (1991) Makromol Chem Makromol Symp 45:205
11. Rohrsetzer S, Wolfram E, Nagy M, Kubicza M (1969) Annales Univ Sci L Eötvös Sect Chimica 11:73
12. Horkay F, Zrinyi M (1985) Macromolecules 15:1306
13. Egle W, Rilk A, Bihr J, Menzel M (1984) Electron Microsc Soc Am Proc 42:566
14. Shaw DJ (1980) Introduction to Colloid and Surface Chemistry. Butterworths & Co Ltd, London-Boston
15. Sonntag H, Strenge K (1987) Coagulation Kinetics and Structure Formation. Plenum Press, New York and London
16. Maeda Y, Hachisu S (1983) Colloids and Surfaces 6:1
17. Zrinyi M, Kabai M, Faix, Horkay F (1988) Progr Coll & Polym Sci 77:165
18. Vicsek T (1989) Fractal Growth Phenomena. World Scientific
19. Meakin P (1988) Advances in Colloid and Interface Science 28:249
20. Julien R, Botet R (1987) Aggregation and Fractal Aggregates. World Scientific Co Pte Ltd
21. Heise B, Kilian H-G, Pietrala M (1977) J Colloid & Polymer Sci 62:16
22. Oka S (1939) Kolloid Z 2:86

Received November 9, 1992;
accepted December 9, 1992

Authors' address:

Prof. Dr. H.G. Kilian
Abt. Experimentelle Physik I
Universität Ulm
Albert-Einstein-Allee 11
89081 Ulm